

Experimental study of the torsion of reinforced concrete members

Constantin E. Chalioris[†]

Democritus University of Thrace, Department of Civil Engineering, Xanthi 671 00, Greece

(Received November 26, 2004, Revised December 2, 2005, Accepted April 18, 2006)

Abstract. This paper presents the results of an experimental investigation on the behaviour of 56 reinforced concrete beams subjected to pure torsion. The reported results include the behaviour curves, the failure modes and the values of the pre-cracking torsional stiffness, the cracking and ultimate torsional moments and the corresponding twists. The influence of the volume of stirrups, the height to width ratios and the arrangement of longitudinal bars on the torsional behaviour is discussed. In order to describe the entire torsional behaviour of the tested beams, the combination of two different analytical models is used. The prediction of the elastic till the first cracking part is achieved using a smeared crack analysis for plain concrete in torsion, whereas for the description of the post-cracking response the softened truss model is used. A simple modification to the softened truss model to include the effect of confinement is also attempted. Calculated torsional behaviour of the tested beams and 21 beams available in the literature are compared with the experimental ones and a very good agreement is observed.

Keywords: angle of twist; beams; reinforced concrete; smeared crack model; softened truss model; stress-strain relationships; torsional stiffness; torsion; torsion tests.

1. Introduction

The experimentally observed torsional behaviour of a reinforced concrete beam comprises two distinct regions; the elastic till the first cracking part and the after cracking part. The different character of the response in these regions reveals the different nature of the load resisting mechanism in each case. Based on this observation, Mitchell and Collins (1974) combined two models to calculate the pre-cracking and post-cracking behaviour (Compression Field Theory) with an abrupt transfer from the first to the second. This theory (known as CFT) has been modified by Vecchio and Collins (1986) to predict the shear response of reinforced concrete beams (Modified Compression Field Theory or MCFT). The main principles of the MCFT have been used in a space truss model to analyse reinforced and prestressed rectangular concrete beams subjected to combined shear, torsion and bending (Rahal and Collins 1995, 2003). This well-known space truss model also checks the possibility of spalling of the concrete cover, considers stress-strain relationships of cracked concrete and provides full and rational behavioural curves that fit well with experimental data.

A non-iterative simplified method for the estimation of the torque capacity of reinforced and

[†] Civil Engineer, MSc, PhD, Lecturer, E-mail: chaliori@civil.duth.gr

prestressed concrete members that is based on the spalled truss model has also been proposed by Rahal and Collins (1996). Extensive comparisons between analytical and measured torsional capacities showed a very good agreement.

The other well-known space truss model with softening of concrete for the problem of torsion of reinforced concrete beams has been first developed by Hsu and Mo in 1985. The softened truss theory has been modified and unified for reinforced and prestressed concrete elements under shear and torsion (Hsu 1993, 1996). Application of this model to reinforced concrete beams under torsion exhibits very reliable results for the prediction of the post-cracking behaviour and the ultimate torque. It is experimentally verified that it can predict the ultimate torsional strength, the angle of twist, the steel and concrete strains throughout the post-cracking torsional response of reinforced concrete beams assuming that the section is cracked from the beginning.

Extensions on the softened truss model have also been proposed in order to predict the torsional capacity of high-strength concrete deep beams (Ashour *et al.* 1999) and reinforced fibrous concrete beams (Mansur *et al.* 1989). Application of the softened truss theory in prestressed high-strength concrete beams under torsion has also been carried out (Wafa *et al.* 1995). Calculated torque curves are compared with experimental ones in all these studies and promising results have been obtained. However, deficiency of the softened truss model consists the fact that predictions of the elastic stiffness of analytical torque - twist curves lies considerable below the test curves in all the examined cases in the literature (Hsu and Mo 1985, Mansur *et al.* 1989, Wafa *et al.* 1995, Ashour *et al.* 1999, Chalioris 1999, 2003).

The elastic torsional behaviour till the development of the first cracks of concrete of a reinforced concrete element is characterized by the high value of torsional stiffness. The influence of reinforcement is of minor importance and the element behaves quite similar to a plain concrete member (Hsu 1993). Thus, the ultimate torque moment of a plain concrete element is approximately equal to the torque moment at cracking of the same element with longitudinal bars and stirrups. The classical Saint Venant theory to the torsion problem of plain concrete members, although it properly describes the elastic behaviour, fails to predict the ultimate torsional strength even in the case of plain concrete.

Recently, a new method for the analysis of plain concrete elements in torsion has been proposed by Karayannidis (2000a). This approach uses an efficient numerical scheme for the torsional analysis of concrete that although initially is based on the elastic theory, it utilizes a special numerical technique properly modified to include the smeared cracking approach. Extensive comparisons between analytical results yielded by this smeared crack analysis and experimental data derived from a broad range of parametrical studies established the validity of this analytical model (Chalioris 1999, Karayannidis 2000b, Karayannidis and Chalioris 2000a, 2000b).

This paper reports experimental results of tests on 56 beam specimens subjected to pure torsion. The reported results comprise entire torsional behavioural curves, failure modes and the values of the initial torsional stiffness, the cracking and ultimate torsional moments and the corresponding angles of twist. The experimental program includes reinforced concrete beams of rectangular cross-section that comprise various longitudinal and transverse reinforcement ratios. Tests of plain concrete beams used as control specimens and beams without transverse reinforcement were also conducted. The influence of various parameters on the torsional behaviour, such as the volume of stirrups and the location of longitudinal steel bars are also reported.

Furthermore, the combination of two analytical models is adopted in order to describe the entire torsional behaviour of reinforced concrete elements. The prediction of the elastic behaviour and the

estimation of the torque moment at cracking are achieved using the smeared crack analysis for plain concrete in torsion (Karayannis 2000a), whereas for the description of the post-cracking response and the calculation of the ultimate torque moment the softened truss model developed by Hsu and Mo (Hsu and Mo 1985, Hsu 1993, 1996) is used. A limited extension to the softened truss model in order to include the effect of confinement is also attempted. Analyses for the prediction of the torsional behaviour of the tested beams and 21 supplementary reinforced concrete beams available in the literature using the proposed combined approach were performed. Calculated torsional behaviour curves are compared with the experimental ones.

2. Research significance

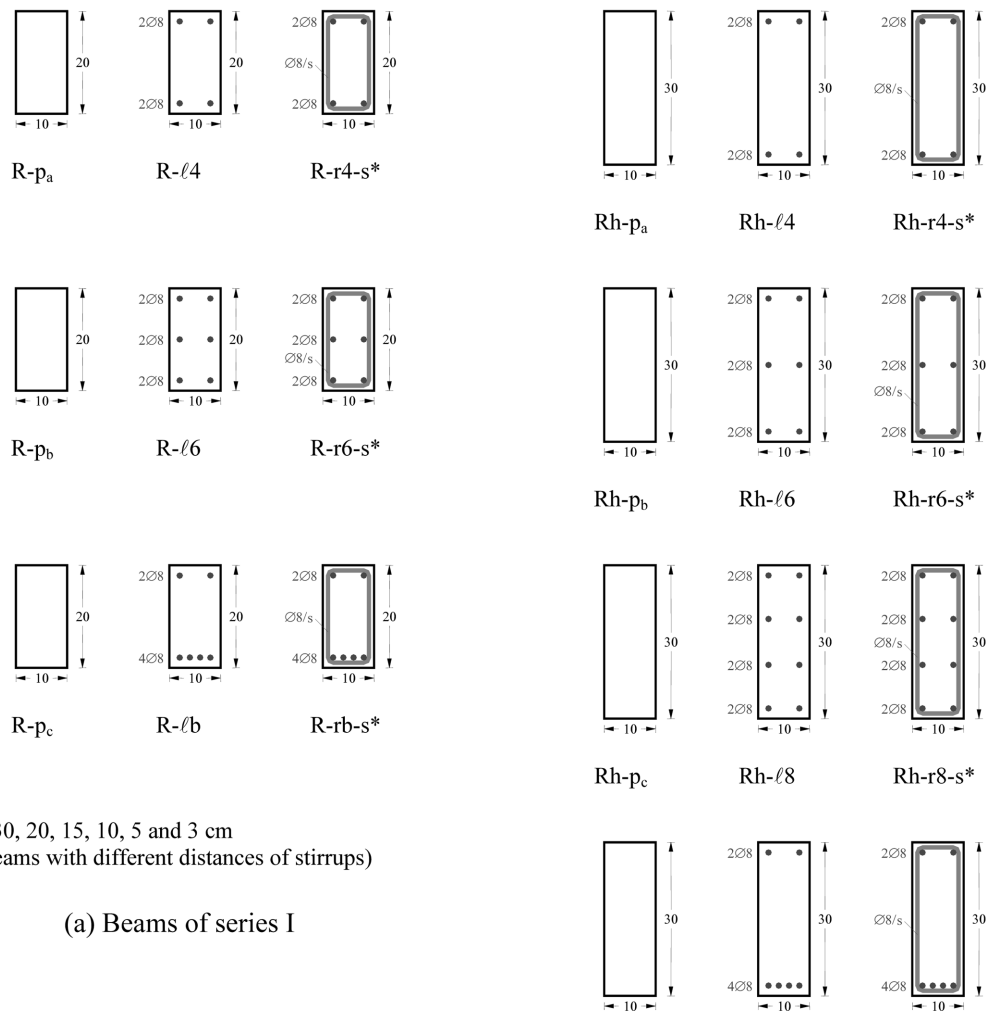
The research presented in this paper provides the literature with experimental curves yielded from torsional tests of 56 reinforced concrete beams with various longitudinal and transverse reinforcement ratios, height to width ratios and reinforcement arrangements. For the prediction of the elastic till the first cracking response of reinforced concrete elements, a smeared crack model is adopted based on the justified assumption that this part of the response is quite similar to the torsional behaviour of plain concrete elements. Further, for the post-cracking response, the well-established softened truss model is used. Despite the fact that these methods are verified, analytical curves that rationally predict the entire torsional response of reinforced concrete members are limited. This work presents a combined approach for the estimation of the entire response, addresses a simple modification to the softened truss model in order to take into account the developed confinement and provides extensive comparisons between analytical and experimental curves of reinforced concrete beams subjected to torsion. The accuracy of the proposed model is also tested on experimental results of the literature.

3. Experimental program

The experimental program comprises fifty-six beams of rectangular cross-section sorted in two series (series I and II) and tested under pure torsion. The main variables were the height to width ratio, the longitudinal and the transverse reinforcement ratios and the arrangement of the longitudinal steel bars of the beams.

3.1 Specimen characteristics

The cross-section dimensions of 24 beams (series I) were 100/200 mm (height to width ratio $h/b = 2$), whereas the other 32 beams (series II) had cross-section dimensions 100/300 mm ($h/b = 3$). The specimens of series I are divided into three groups (R4, R6 and Rb) and the specimens of series II are divided into four groups (Rh4, Rh6, Rh8 and Rhb). Each group comprises eight specimens; one of them is a plain concrete beam (control specimen without reinforcement), one has only longitudinal reinforcement (deformed bars) and the other six specimens have longitudinal and transverse reinforcement (deformed longitudinal bars and plain stirrups). The transverse reinforcement used in these six specimens was 8 mm diameter closed stirrups at a uniform spacing of 300 mm, 200 mm, 150 mm, 100 mm, 50 mm and 30 mm, respectively for each beam. Steel



(a) Beams of series I

* s = 30, 20, 15, 10, 5 and 3 cm
(six beams with different distances of stirrups)

(b) Beams of series II

Fig. 1 Cross-section and reinforcement arrangement of the tested beams

yield strength was 518 MPa for longitudinal steel bars and 365 MPa for mild steel stirrups.

The longitudinal reinforcement used in the beams of groups R4 and Rh4 was four longitudinal bars of diameter 8 mm ($4\varnothing 8$) at the corners of the closed stirrups. The longitudinal reinforcement of beams of groups R6 and Rh6 comprised $6\varnothing 8$; four of them at the corners of the stirrups and the other two bars at the midheight of the closed stirrups (total longitudinal reinforcement $6\varnothing 8$ uniformly distributed). Beams of groups Rb and Rhb had also four bars $\varnothing 8$ at the corners of the stirrups and two additional bars $\varnothing 8$ at the bottom side of the closed stirrups. Thus, the total

Table 1 Series I - Reinforcement and concrete strength

Group	Beams code name	Longitudinal bars	Stirrups	ρ_ℓ (%)	ρ_t (%)	f'_c (MPa)	f'_{sp} (MPa)
R4	R-p _a	—	—	—	—		
	R-ℓ4		—		—		
	R-r4-30	4Ø8 total:	Ø8/300		0.41		
	R-r4-20		Ø8/200		0.61	20.96	2.89
	R-r4-15	2Ø8 top	Ø8/150	1.01	0.82		
	R-r4-10	2Ø8 bottom	Ø8/100		1.23		
	R-r4-5	(4 corner bars)	Ø8/50		2.45		
R6	R-r4-3		Ø8/30		4.09		
	R-p _b	—	—	—	—		
	R-ℓ6		—		—		
	R-r6-30	6Ø8 total:	Ø8/300		0.41		
	R-r6-20	2Ø8 top	Ø8/200		0.61	24.59	3.33
	R-r6-15	2Ø8 middle	Ø8/150	1.51	0.82		
	R-r6-10	2Ø8 bottom	Ø8/100		1.23		
Rb	R-r6-5	(6 uniformly distributed bars)	Ø8/50		2.45		
	R-r6-3		Ø8/30		4.09		
	R-p _c	—	—	—	—		
	R-ℓb		—		—		
	R-rb-30	6Ø8 total:	Ø8/300		0.41		
	R-rb-20		Ø8/200		0.61	24.07	2.98
	R-rb-15	2Ø8 top	Ø8/150	1.51	0.82		
	R-rb-10	4Ø8 bottom	Ø8/100		1.23		
	R-rb-5	(6 unsymmetrical bars)	Ø8/50		2.45		
	R-rb-3		Ø8/30		4.09		

longitudinal reinforcement of these beams consisted of 2Ø8 top and 4Ø8 bottom at the cross-section (unsymmetrical bending type of longitudinal reinforcement). Finally, the longitudinal reinforcement used in the beams of group Rh8 was eight bars of diameter 8 mm (8Ø8); four of them at the corners of the stirrups and the other four bars were uniformly distributed at the height of stirrups sides. Geometrical and reinforcement arrangement details for the tested beams of series I are presented in Fig. 1(a) and Table 1, whereas for beams of series II in Fig. 1(b) and Table 2.

The code names of the tested beams presented in Tables 1 and 2 and Fig. 1 comprise two or three parts of digits. The first represents the cross-section of the beams: "R" for the beams that $h = 200$ mm and "Rh" for the beams that $h = 300$ mm. The second part shows the type of the reinforcement: "p" for the plain concrete beams without reinforcement (control specimens), "ℓ" for the beams with longitudinal only reinforcement and "r" for the beams with bars and stirrups. After the digit "ℓ" or "r", the number "4", "6" or "8" indicates the number of the longitudinal bars, whereas the letter "b" indicates the unsymmetrical longitudinal reinforcement (bending type of reinforcement). The superscripts of the digit "p" show that the experimental program includes one plain beam as control specimen for each group. Finally, the third part of the beams' name is a number that appears only

Table 2 Series II - Reinforcement and concrete strength

Group	Beams code name	Longitudinal bars	Stirrups	ρ_ℓ (%)	ρ_t (%)	f'_c (MPa)	f'_{sp} (MPa)
Rh4	Rh-p _a	—	—	—	—		
	Rh-ℓ4		—		—		
	Rh-r4-30	4Ø8 total:	Ø8/300		0.38		
	Rh-r4-20		Ø8/200		0.58	26.56	3.04
	Rh-r4-15	2Ø8 top	Ø8/150	0.67	0.77		
	Rh-r4-10	2Ø8 bottom	Ø8/100		1.15		
	Rh-r4-5	(4 corner bars)	Ø8/50		2.31		
	Rh-r4-3		Ø8/30		3.84		
Rh6	Rh-p _b	—	—	—	—		
	Rh-ℓ6		—		—		
	Rh-r6-30	6Ø8 total:	Ø8/300		0.38		
	Rh-r6-20	2Ø8 top	Ø8/200		0.58	24.90	3.42
	Rh-r6-15	2Ø8 middle	Ø8/150	1.01	0.77		
	Rh-r6-10	2Ø8 bottom	Ø8/100		1.15		
	Rh-r6-5	(6 uniformly distributed bars)	Ø8/50		2.31		
	Rh-r6-3		Ø8/30		3.84		
Rh8	Rh-p _c	—	—	—	—		
	Rh-ℓ8		—		—		
	Rh-r8-30	8Ø8 total:	Ø8/300		0.38		
	Rh-r8-20	2Ø8 top	Ø8/200		0.58	27.39	3.09
	Rh-r8-15	4Ø8 middle	Ø8/150	1.34	0.77		
	Rh-r8-10	2Ø8 bottom	Ø8/100		1.15		
	Rh-r8-5	(8 uniformly distributed bars)	Ø8/50		2.31		
	Rh-r8-3		Ø8/30		3.84		
Rhb	Rh-p _d	—	—	—	—		
	Rh-ℓb		—		—		
	Rh-rb-30	6Ø8 total:	Ø8/300		0.38		
	Rh-rb-20		Ø8/200		0.58	24.49	2.89
	Rh-rb-15	2Ø8 top	Ø8/150	1.01	0.77		
	Rh-rb-10	4Ø8 bottom	Ø8/100		1.15		
	Rh-rb-5	(6 unsymmetrical bars)	Ø8/50		2.31		
	Rh-rb-3		Ø8/30		3.84		

after the digit "r" (in beams with bars and stirrups) and equals the spacing of the stirrups in centimetres.

The cement used in this experimental work was a locally manufactured general purpose ordinary Portland type cement (type 35IIa, Greek type pozzolan cement). Sand with a high fineness modulus and coarse aggregates with a maximum size of 9.5 mm (3/8 in.) were used. The concrete mixture was made using cement, sand and crushed aggregates in a proportion 1:2.8:1.2, respectively, and

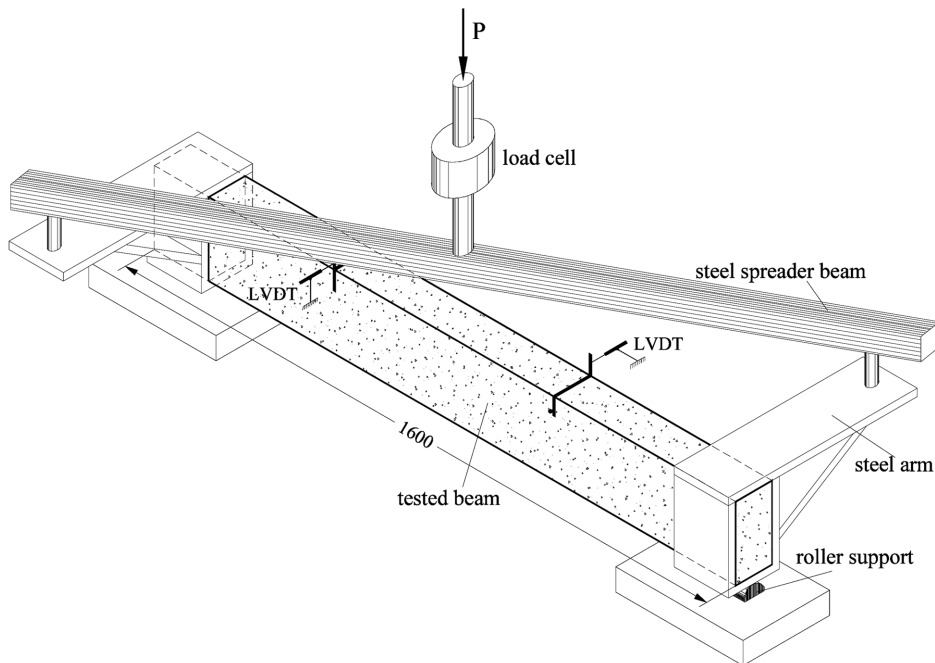


Fig. 2 Test setup and specimen configuration

water to cement ratio equal to 0.43. Also included in Tables 1 and 2 are the concrete compressive and tensile strength values as measured from supplementary compression and splitting tests, respectively. Reported strength values are averages from three standard 150×300 mm cylinders for each case and group of specimens.

3.2 Test setup and test procedure

The total length in all beam specimens was 1.60 m. The experimental setup is shown in Fig. 2. The specimens were supported on two roller supports 1.30 m apart. These supports ensured that the test beam was free to twist and to elongate longitudinally at both ends. The load was applied on the ends of two steel arms fixed at the end parts of each tested beam, through a steel spreader as shown in Fig. 2. These end parts of the tested beams were properly over-reinforced so that they can support without cracking the imposed loading. The test region was the central 800 mm of the specimens.

The load was imposed consistently in low rate (approximately 0.001 rad/min for the pre-cracking part and for the plain concrete beams and 0.005 rad/min after the full cracking of concrete) and was measured by a load cell with accuracy equal to 0.025 kN. The average angle of twist per unit length of the tested beams was estimated using the measurements of two linear variable differential transducers (LVDTs) with high accuracy (0.001 mm). These two LVDTs measured the opposite deformations of each specimen as it rotates and were placed 600 mm apart as shown in Fig. 2. In order to acquire useful information about the failure modes of the tested beams, the strains of the longitudinal and transverse steel reinforcements were measured by electrical resistance strain gauges. Two strain gauges were mounted on each longitudinal bar and on the stirrups at midspan at

the effective central span of the beams. Measurements for load, deformations and steel strains were read and recorded continuously through a data acquisition system.

The beams were tested in monotonically increasing torque moment until the value of the ultimate torsional capacity is reached then in increasing twist until the total failure of the specimen or until the maximum twist capacity of the test setup.

4. Test results and discussions

The measured initial pre-cracking torsional stiffness ($K_{cr,exp}$), torque moment at cracking ($T_{cr,exp}$) and angle of twist per unit length at cracking ($\vartheta_{cr,exp}$), ultimate torque moment ($T_{u,exp}$) and corresponding

Table 3 Series I - Test results

Beams code name	Pre-cracking			Post-cracking		Failure mode
	$T_{cr,exp}$ (kN·m)	$\vartheta_{cr,exp}$ (rad/m)	K_{exp} (†)	$T_{u,exp}$ (kN·m)	$\vartheta_{T_{u,exp}}$ (rad/m)	
R-p _a	1.934	0.009	3079	*	*	CC
R-ℓ4	2.098	0.007	3558	*	*	LL
R-r4-30	2.115	0.008	3449	*	*	T
R-r4-20	2.171	0.008	3771	2.385	0.051	T
R-r4-15	2.013	0.008	3084	2.649	0.074	T
R-r4-10	2.008	0.009	3229	3.254	0.099	C
R-r4-5	2.306	0.009	3483	3.974	0.115	C
R-r4-3	3.058	0.011	3512	4.172	0.089	C
R-p _b	2.325	0.010	3434	*	*	CC
R-ℓ6	2.514	0.012	3222	*	*	LL
R-r6-30	2.407	0.009	3402	2.640	0.013	T
R-r6-20	2.401	0.009	3452	2.873	0.064	T
R-r6-15	2.596	0.011	3557	3.184	0.073	T
R-r6-10	2.646	0.011	3442	3.742	0.078	T
R-r6-5	2.423	0.009	3313	4.251	0.079	C
R-r6-3	2.790	0.011	3602	4.443	0.072	C
R-p _c	2.049	0.009	3200	*	*	CC
R-ℓb	2.068	0.008	3086	*	*	LL
R-rb-30	2.229	0.009	3288	*	*	T
R-rb-20	2.162	0.008	3829	2.452	0.040	T
R-rb-15	2.360	0.009	3303	3.116	0.055	T
R-rb-10	2.621	0.010	3342	3.702	0.049	T
R-rb-5	2.696	0.012	3476	4.163	0.055	C
R-rb-3	2.559	0.010	2945	4.347	0.063	C

*: ultimate torsional moment and corresponding angle of twist are equal to the observed torsional moment and angle of twist at cracking

†: $\times 10^{-7}$ kN · m²/rad

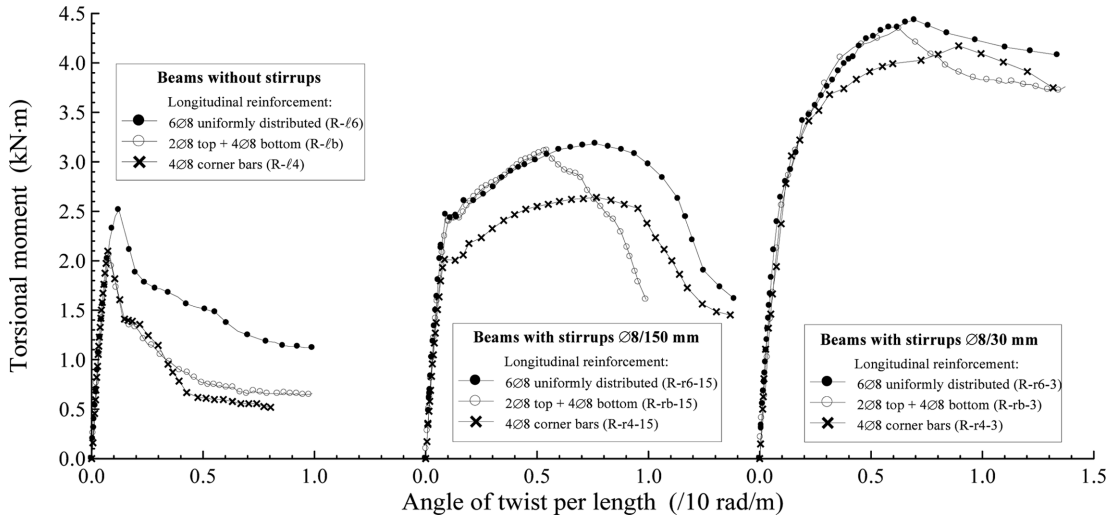
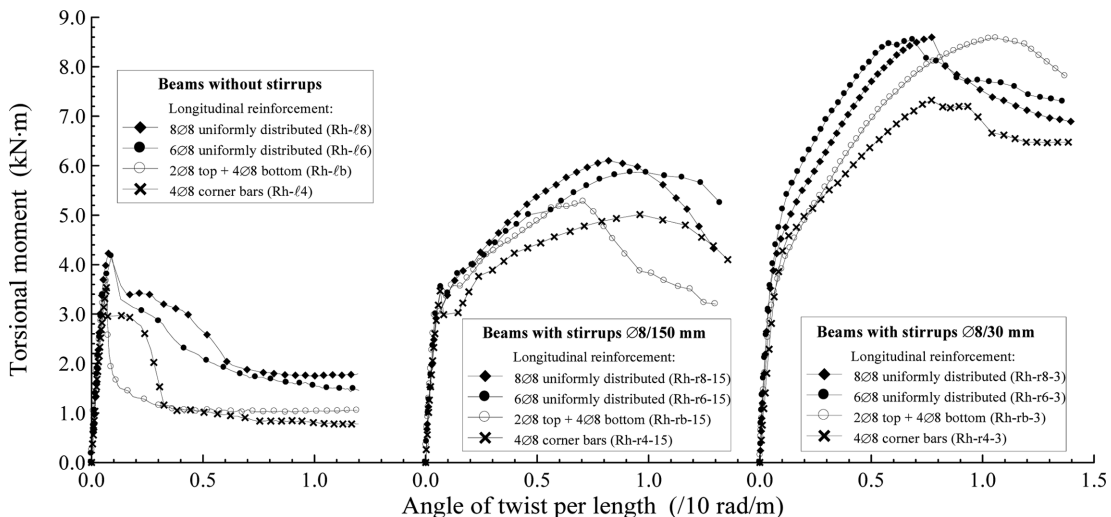
angle of twist per unit length ($\vartheta_{Tu,exp}$) are presented in Tables 3 and 4. The typical torsional behaviour of tested beams of series I and II are also presented in Figs. 3 and 4, respectively, in terms of torque moment (T) versus angle of twist per unit length (ϑ) experimental curves. In order to facilitate comparison, T - ϑ curves of each figure are divided in three groups so that beams of the

Table 4 Series II - Test results

Beams code name	Pre-cracking			Post-cracking		Failure mode
	$T_{cr,exp}$ (kN·m)	$\vartheta_{cr,exp}$ (rad/m)	K_{exp} (\dagger)	$T_{u,exp}$ (kN·m)	$\vartheta_{Tu,exp}$ (rad/m)	
Rh-p _a	3.376	0.007	6040	*	*	CC
Rh- ℓ 4	3.519	0.007	6604	*	*	LL
Rh-r4-30	3.656	0.007	6314	*	*	LT
Rh-r4-20	3.220	0.007	5913	3.948	0.077	LT
Rh-r4-15	3.645	0.008	6689	5.013	0.096	LT
Rh-r4-10	4.188	0.008	6186	5.834	0.107	LT
Rh-r4-5	3.654	0.008	6339	7.144	0.072	L
Rh-r4-3	3.349	0.006	5712	7.331	0.078	L
Rh-p _b	3.792	0.007	6410	*	*	CC
Rh- ℓ 6	4.170	0.009	7132	*	*	LL
Rh-r6-30	3.952	0.006	8144	4.241	0.081	T
Rh-r6-20	3.787	0.007	6494	4.811	0.085	T
Rh-r6-15	3.551	0.007	7215	5.869	0.090	T
Rh-r6-10	3.721	0.007	6755	6.616	0.088	T
Rh-r6-5	4.343	0.009	9273	8.474	0.108	C
Rh-r6-3	4.977	0.010	9420	8.559	0.068	C
Rh-p _c	3.378	0.006	6964	*	*	CC
Rh- ℓ 8	4.237	0.010	7737	*	*	LL
Rh-r8-30	3.650	0.008	8281	4.464	0.072	T
Rh-r8-20	3.453	0.008	7744	5.037	0.074	T
Rh-r8-15	3.304	0.006	7191	6.120	0.085	T
Rh-r8-10	3.683	0.009	6658	6.950	0.096	T
Rh-r8-5	3.921	0.008	7517	8.553	0.093	C
Rh-r8-3	4.163	0.007	9113	8.594	0.077	C
Rh-p _d	3.313	0.006	6530	*	*	CC
Rh- ℓ b	3.706	0.007	7292	*	*	LL
Rh-rb-30	3.898	0.006	8837	*	*	T
Rh-rb-20	3.181	0.007	7616	4.308	0.085	LT
Rh-rb-15	3.209	0.005	7844	5.327	0.072	LT
Rh-rb-10	3.284	0.008	6963	6.543	0.106	LT
Rh-rb-5	3.812	0.009	7260	8.300	0.129	L
Rh-rb-3	3.794	0.009	7445	8.581	0.106	L

*: ultimate torsional moment and corresponding angle of twist are equal to the observed torsional moment and angle of twist at cracking

\dagger : $\times 10^{-7}$ kN · m²/rad

Fig. 3 Typical experimental T - θ curves for beams of series IFig. 4 Typical experimental T - θ curves for beams of series II

same group comprise the same transverse reinforcement and different longitudinal reinforcement volume and arrangement.

Based on the crack patterns and the measurements of the strains of the longitudinal and transverse steel reinforcement the following failure modes have been observed:

CC: Concrete crushed (absence of reinforcement in plain concrete beams).

LL: Longitudinal steel yielded before concrete crushing (absence of transverse reinforcement in beams with longitudinal bars only).

LT: Longitudinal and transverse steel yielded before concrete crushing (under-reinforced beams).

L : Longitudinal steel yielded before concrete crushing, whereas transverse reinforcement did not yield.

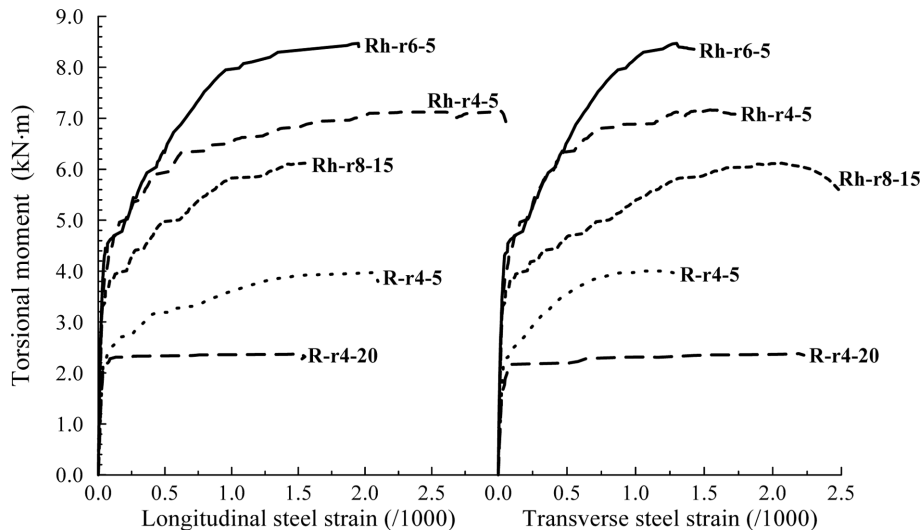


Fig. 5 Typical experimental torque versus steel strain curves

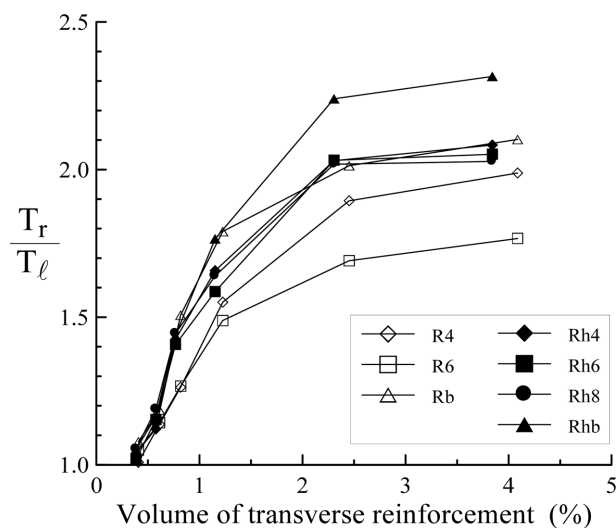


Fig. 6 Effect of the transverse reinforcement on the torque capacity of tested beams

T : Transverse steel yielded before concrete crushing, whereas longitudinal reinforcement did not yield.

C : Concrete crushed before steel bars or stirrups yielding (over-reinforced beams).

The failure mode of each tested beam is presented in Tables 3 and 4. Typical measured curves of torsional moment versus longitudinal and transverse steel strains are also shown in Fig. 5.

In order to estimate the effect of transverse reinforcement on the torsional strength, curves of the ratio of the measured torque capacity of beams reinforced with bars and stirrups (T_r) to the ultimate experimental torque moment of the same beams without stirrups (T_ℓ) versus the volume of the transverse reinforcement are shown in Fig. 6.

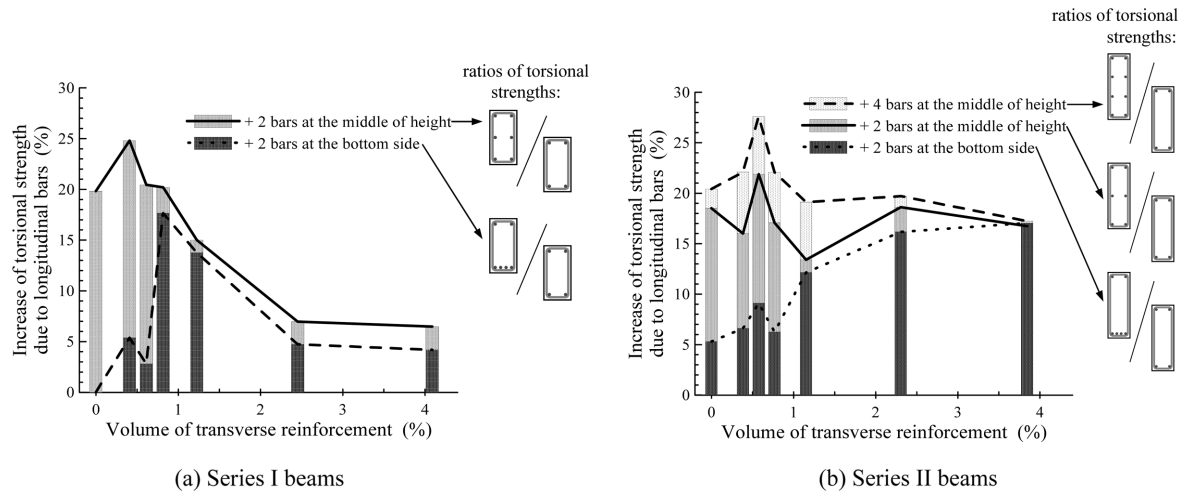


Fig. 7 Increase of torsional strength due to the addition of longitudinal bars

Furthermore, Fig. 7 shows the effect of longitudinal bars volume and their arrangement on the torsional behaviour of the tested beams. This figure presents the percentage increase of the torsional strength due to the addition of (i) two steel bars of diameter 8 mm at the midheight of the closed stirrups (beams of series I and II), (ii) two bars of diameter 8 mm at the bottom side of the stirrups (beams of series I and II) and (iii) four bars of diameter 8 mm uniformly distributed at the height of stirrups sides (beams of series II).

Based on the experimental results reported in Tables 3 and 4 and presented in Figs. 3, 4, 5, 6 and 7 the following can be observed.

Transverse reinforcement strongly affects the torsional behaviour of the tested beams, as it was expected. The torque capacity of the tested beams increased with an increase in the value of volume of transverse reinforcement up to a value of 2.5% for the latter (Fig. 6). Beyond this value the increase of the torsional strength becomes less significant. Similar conclusions were observed by Hsu (1968) and Victor and Muthukrishnan (1973).

The ultimate torsional moment of the tested beams increased due to the addition of longitudinal steel bars. This increase is not proportional to the volume of longitudinal reinforcement and seems to be relative small when the bars were added at the bottom side of the stirrup (unsymmetrical bending type of longitudinal reinforcement arrangement) and the volume of the transverse reinforcement is relatively low (Fig. 7). Further, most of the beams of group R_{hb} (beams with height to width ratio 3 and unsymmetrical longitudinal reinforcement 2Ø8 top and 4Ø8 bottom) exhibited the same failure modes with the beams of group R_h (beams with $h/b = 3$ and 4Ø8 corner bars).

5. Behavioural models

The typical torque moment (T) versus angle of twist (ϑ) experimental curve of a reinforced concrete element, that includes longitudinal bars and stirrups (see for example T - ϑ curve of beam R-4-15 in Fig. 3), comprises two distinct regions; an elastic till the first cracking part and a post-

cracking part. The different character of the response in these regions reveals the different nature of the load resisting mechanism in each case. The pre-cracking part is characterized by the high value of torsional stiffness. The element behaves as a homogeneous one and the influence of reinforcement is of minor importance. The post-cracking part is characterized by a further increase of the torque moment at a lower rate, depending on the volume of the transverse reinforcement. The consistently decreasing torsional stiffness reveals the different nature of the mechanism of resistance. The transition from the one region to the other is abrupt in most of the beams with $\rho_t < 1.5\%$ and is characterized by the lack of a ready bearing mechanism.

Based on the above observation, the combination of two different theories is adopted, as Mitchell and Collins addressed in 1974, in order to describe the entire torsional behaviour of reinforced concrete elements. The elastic till the first cracking part is described by a smeared crack analysis for plain concrete in torsion (Karayannis 2000a) and the post-cracking part is described by the well-known softened truss model (Hsu and Mo 1985, Hsu 1993, 1996).

5.1 Model for the pre-cracking behaviour

It is justified that for the elastic till the first cracking part the percentage of steel has a minor effect on the torsional response and reinforced concrete elements behave as plain concrete members. Therefore, the analytical smeared crack model for plain concrete in torsion proposed by Karayannis (2000a) is applicable to reinforced concrete beams for the prediction of the torsional behaviour till concrete cracking (pre-cracking). This approach is using an efficient numerical scheme for the torsional analysis of concrete that is initially based on the elastic theory and utilizes a special numerical technique properly modified to include the smeared cracking approach.

Based on the theory of Saint Venant and the complimentary approach by Prandtl, the elastic torsional response of a structural element consisting of more than one material (or one homogeneous material that its properties vary over the cross-section) is expressed by

$$\frac{\partial}{\partial x} \left(\frac{1}{G} \frac{\partial F}{\partial x} \right) + \frac{\partial}{\partial y} \left(\frac{1}{G} \frac{\partial F}{\partial y} \right) = -2\vartheta \quad (1)$$

where F = stress function that satisfies all boundary conditions, ϑ = angle of twist per unit length and G = shear modulus of rigidity.

The relationships between the shear stress components τ_{zx} and τ_{zy} that are developed due to torsion, with the function F are

$$\tau_{zx} = \frac{\partial F}{\partial y} \quad \text{and} \quad \tau_{zy} = -\frac{\partial F}{\partial x} \quad (2)$$

and the shear stress at a point is

$$\tau = \sqrt{\tau_{zx}^2 + \tau_{zy}^2} \quad (3)$$

Since only shear stresses develop on a cross-section of an element subjected to pure torsion without skew restraint, an infinitesimal element on this cross-section is in pure shear stress state. Thus, considering an infinitesimal element in pure shear stress state it can be deduced that in the case of pure torsion the response can be characterized by the behaviour of the material in direct tension with tensile stress equal to the developing shear stress.

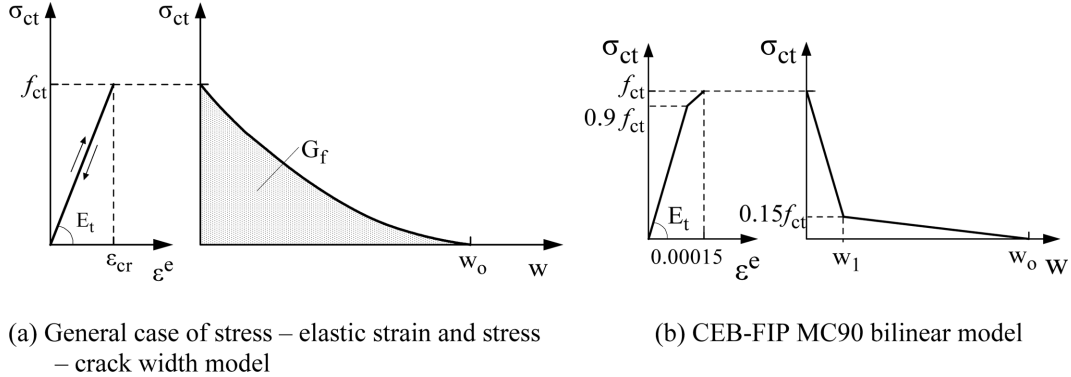


Fig. 8 Tensile behaviour of concrete

The model of Karayannidis (2000a) is based on the observation that, in reality, tensile concrete cracking consists of systems of parallel cracks that are continuously distributed over the concrete mass. Cracks are considered to be adequately represented by parallel microcracks distributed (smeared) over the finite elements. That is, cracks are merely represented as a change in the material property of the element over which the cracks are assumed to be smeared. Thus, crack propagation takes place with the formation of a fracture process zone (crack band) that is defined as the boundary of the strain softening region that is caused not only by microcracking but also by any bond ruptures, so the fracture process zone is assumed wider than the region of visible microcracks.

The analytical technique of this method employs constitutive relations expressed in terms of normal tensile stress and crack width for the behaviour of this crack process zones. The width ℓ_w of this fracture process zone is considered as a material property that, except for the influence of the stress distribution, mainly depends on the nature and the size of the aggregates and the other ingredients of concrete.

The energy required for the formation of all microcracks of the crack band and fully opening of one single crack for a unit area crack plane is the fracture energy G_f . The fracture energy in terms of the area under the curve of concrete tensile stress σ_{ct} versus crack width w (see Fig. 8a) is

$$G_f = \int_{\sigma_{ct} = f_{ct}}^0 \sigma_{ct} dw \quad (4)$$

Between the microcracks of the fracture process zone there are less damaged or even elastic parts. Thus, the total concrete tensile strain ε_{ct} can be considered as the sum of an elastic ε^e and a fracture ε^{fr} strain component. In the general case for any relationship between σ_{ct} and w is

$$\varepsilon_{ct} = \varepsilon^e + \varepsilon^{fr} = \frac{\sigma_{ct}}{E_{ct}} + f_w(\sigma_{ct}) \quad (5)$$

where E_{ct} = the modulus of elasticity of concrete and the fracture component ε^{fr} is a function of the stress $f_w(\sigma_{ct})$ with average value over the front of the crack band equal to w/ℓ_w .

The crack width for a fully opened crack w_o is determined from Eq. (4) as

$$w_o = \alpha_f \frac{G_f}{f_{ct}} \quad (6)$$

where α_f = coefficient that depends on the shape of the $\sigma_{ct} - w$ curve and the nature and the size of the concrete aggregates. For a linear $\sigma_{ct} - w$ curve $\alpha_f = 2$, whereas for the bilinear curve defined by CEB MC90 $\alpha_f = 5$ to 8 (Fig. 8b).

The method is also applicable to concrete elements subjected to torsion combined with flexure, shear and axial force (Karayannis and Chalioris 2000b) and can easily be applied to elements with arbitrary cross-section since it includes numerical mapping and it has no need of extended computing power because it does not make use of any stiffness matrix calculations. The analysis can be considered as a combination of fracture mechanics and numerical analysis.

Details of this analytical model and its applications are presented in the references (Karayannis 2000a, Karayannis and Chalioris 2000b). Further, detailed verification of the model has been achieved through extensive comparisons between calculated and experimental results derived from a broad range of parametrical studies (Karayannis and Chalioris 2000a).

5.2 Model for the post-cracking behaviour

Among the various theories available in the literature, researchers have a common consensus that the space truss models (the spalled and the softened truss model) are the most rational and powerful models for dealing with torsional problems. In the present study, the theory of the softened truss model (Hsu and Mo 1985, Hsu 1993, 1996) is used.

The method relies on solving three equilibrium and three compatibility equations along with the constitutive laws of an element taken from a member subjected to pure torsion. The equations of equilibrium and compatibility are based on the assumption that the material is continuous. Thus, all derived stress and strains have to be average stresses and strains, respectively. As a result, the constitutive laws of concrete and steel must relate the average stresses to the average strains of each material. Detailed derivation of the equations and the solution technique of this theory can be found in the well-known studies of Hsu and Mo (1985) and Hsu (1993, 1996).

Especially for the concrete in compression, taking into account the fact that concrete struts strength is greatly reduced by the diagonal cracking caused by tension in the perpendicular direction (concrete softening), the following constitutive laws have been formulated (Hsu 1993, 1996, Belarbi and Hsu 1995)

if $\varepsilon_d \leq \zeta \varepsilon_o$

$$\sigma_d = \zeta f'_c \left[2 \frac{\varepsilon_d}{\zeta \varepsilon_o} - \left(\frac{\varepsilon_d}{\zeta \varepsilon_o} \right)^2 \right] \quad (7)$$

and when $\varepsilon_d > \zeta \varepsilon_o$

$$\sigma_d = \zeta f'_c \left[1 - \left(\frac{\varepsilon_d / (\zeta \varepsilon_o) - 1}{2/\zeta - 1} \right)^2 \right] \quad (8)$$

where ζ is the softening coefficient taken as

$$\zeta = \frac{0.9}{\sqrt{1 + 400 \varepsilon_r}} \quad (9)$$

In the present work a limited extension of the softened truss model is attempted in order to describe the behaviour of reinforced concrete beams with high volume of transverse reinforcement.

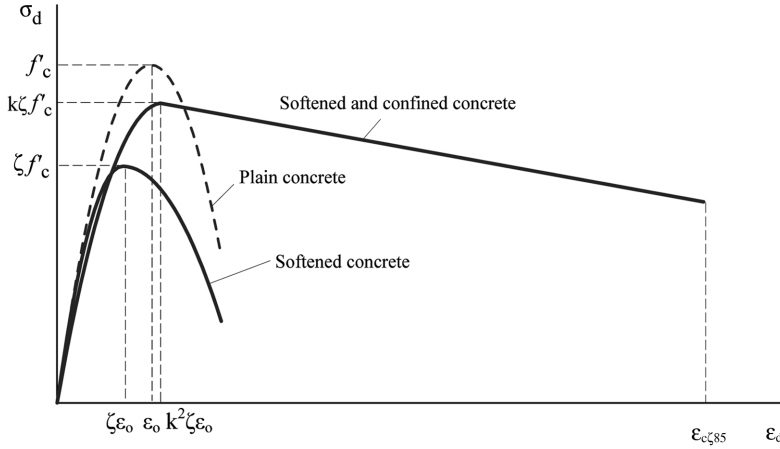


Fig. 9 Concrete compressive stress versus strain curves

In these cases (beams of the experimental program with stirrups $\varnothing 8/50$ mm and $\varnothing 8/30$ mm) it is proposed to take into account the developed confinement of concrete due to the short spacing of stirrups. Thus, the proposed compressive stress versus strain curve for softened and confined concrete can be defined as a parabolic equation until the point of ultimate stress and after that point the curve is linearly reduced until the point of ultimate strain ($0.85\zeta f'_c$, $\varepsilon_{c\zeta85}$) (Fig. 9):

if $\varepsilon_d \leq k^2\zeta\varepsilon_0$

$$\sigma_d = k\zeta f'_c \left[2 \frac{\varepsilon_d}{k^2\zeta\varepsilon_0} - \left(\frac{\varepsilon_d}{k^2\zeta\varepsilon_0} \right)^2 \right] \quad (10)$$

and when $\varepsilon_d > k^2\zeta\varepsilon_0$

$$\varepsilon_{c\zeta85} = \varepsilon_{\zeta85} + 0.1 \cdot \alpha \cdot \omega_w \quad (11)$$

where

k = confinement index taken as (CEB-FIP MC90 1993)

$$\text{if } \alpha \cdot \omega_w \leq 0.1 \quad k = 1 + 2.5 \cdot \alpha \cdot \omega_w \quad (12)$$

$$\text{and when } \alpha \cdot \omega_w > 0.1 \quad k = 1.125 + 1.25 \cdot \alpha \cdot \omega_w \quad (13)$$

α = confinement empirical coefficient (= 0.18 for the case of one stirrup, CEB-FIP MC90)

ω_w = mechanical ratio taken as

$$\omega_w = \frac{\text{volume of stirrup}}{\text{volume of the confined core}} \cdot \frac{f_{yt}}{f'_c} \quad (14)$$

$\varepsilon_{\zeta85}$ = softened concrete strain at compressive stress equal to $0.85\zeta f'_c$ and Eq. (8) gives

$$\varepsilon_{\zeta85} = (0.775 + 0.613\zeta)\varepsilon_0 \quad (15)$$

Table 5 Calculated results and comparisons with the measured ones

Beams code name	Pre-cracking				Post-cracking		
	$T_{cr, cal}$ (kN·m)	$\frac{T_{cr, exp}}{T_{cr, cal}}$	K_{cal} (†)	$\frac{K_{exp}}{K_{cal}}$	$T_{u, cal}$ (kN·m)	$\frac{T_{u, exp}}{T_{u, cal}}$	$\vartheta_{Tu, cal}$ (rad/m)
R-p _a	0.95		0.92	—	—	—	—
R-ℓ4	1.03		1.06	—	—	—	—
R-r4-30	1.03		1.03	—	—	—	—
R-r4-20	1.06		1.13	2.633	0.91	0.099	
R-r4-15	2.047	0.98	3346	0.92	2.775	0.95	0.096
R-r4-10		0.98		0.97	2.923	1.11	0.091
R-r4-5		1.13		1.04	4.103*	0.97	0.135*
R-r4-3		1.49		1.05	4.165*	1.00	0.133*
R-p _b	0.99		0.95	—	—	—	—
R-ℓ6	1.07		0.89	—	—	—	—
R-r6-30	1.02		0.94	—	—	—	—
R-r6-20	1.02		0.95	2.888	0.99	0.080	
R-r6-15	2.359	1.10	3624	0.98	3.228	0.99	0.094
R-r6-10		1.12		0.95	3.467	1.08	0.090
R-r6-5		1.03		0.91	4.995*	0.85	0.131*
R-r6-3		1.18		0.99	5.131*	0.87	0.124*
Rh-p _a	1.00		0.93	—	—	—	—
Rh-ℓ4	1.04		1.02	—	—	—	—
Rh-r4-30	1.08		0.97	—	—	—	—
Rh-r4-20	0.95		0.91	4.400	0.90	0.097	
Rh-r4-15	3.378	1.08	6500	1.03	5.009	1.00	0.101
Rh-r4-10		1.24		0.95	5.250	1.11	0.099
Rh-r4-5		1.08		0.98	6.916*	1.03	0.104*
Rh-r4-3		0.99		0.88	7.103*	1.03	0.095*
Rh-p _b	1.00		1.02	—	—	—	—
Rh-ℓ6	1.10		1.13	—	—	—	—
Rh-r6-30	1.04		1.29	—	—	—	—
Rh-r6-20	1.00		1.03	4.442	1.08	0.081	
Rh-r6-15	3.800	0.93	6292	1.15	5.099	1.15	0.093
Rh-r6-10		0.98		1.07	5.416	1.22	0.089
Rh-r6-5		1.14		1.47	7.618*	1.11	0.135*
Rh-r6-3		1.31		1.50	7.753*	1.10	0.127*
Rh-p _c	0.98		1.06	—	—	—	—
Rh-ℓ8	1.23		1.17	—	—	—	—
Rh-r8-30	1.06		1.26	—	—	—	—
Rh-r8-20	1.01		1.17	4.622	1.09	0.072	
Rh-r8-15	3.434	0.96	6596	1.09	5.511	1.11	0.081
Rh-r8-10		1.07		1.01	6.037	1.15	0.087
Rh-r8-5		1.14		1.14	8.657*	0.99	0.125*
Rh-r8-3		1.21		1.38	8.893*	0.97	0.127*
Mean:	1.070	—	1.057	—	1.031	—	
Standard deviation:	0.111	—	0.150	—	0.096	—	

*: using the modified softened truss model that includes the confinement effect

†: $\times 10^{-7}$ kN · m²/rad

6. Analytical predictions and comparisons with test results

Analyses for the calculation of the torsional behaviour of the tested beams using the proposed combined approach were performed. Smeared crack analysis was performed for all the tested specimens (7 plain and 49 reinforced concrete beams) in order to determine the elastic and the pre-cracking response, the torsional moment and the twist at cracking. The softened truss model for the post-cracking part was performed for 25 specimens that evince post-cracking behaviour (reinforced concrete beams with bars and stirrups spacing 200, 150, 100, 50 and 30 mm) and comprise uniformly distributed longitudinal bars (groups R4, R6, Rh4, Rh6 and Rh8). It is mentioned that from these 25 specimens, in 10 beams with stirrups $\varnothing 8/50$ mm and $\varnothing 8/30$ mm, the softened truss model with the effect of the confinement was also performed in order to estimate the effectiveness of the proposed modification.

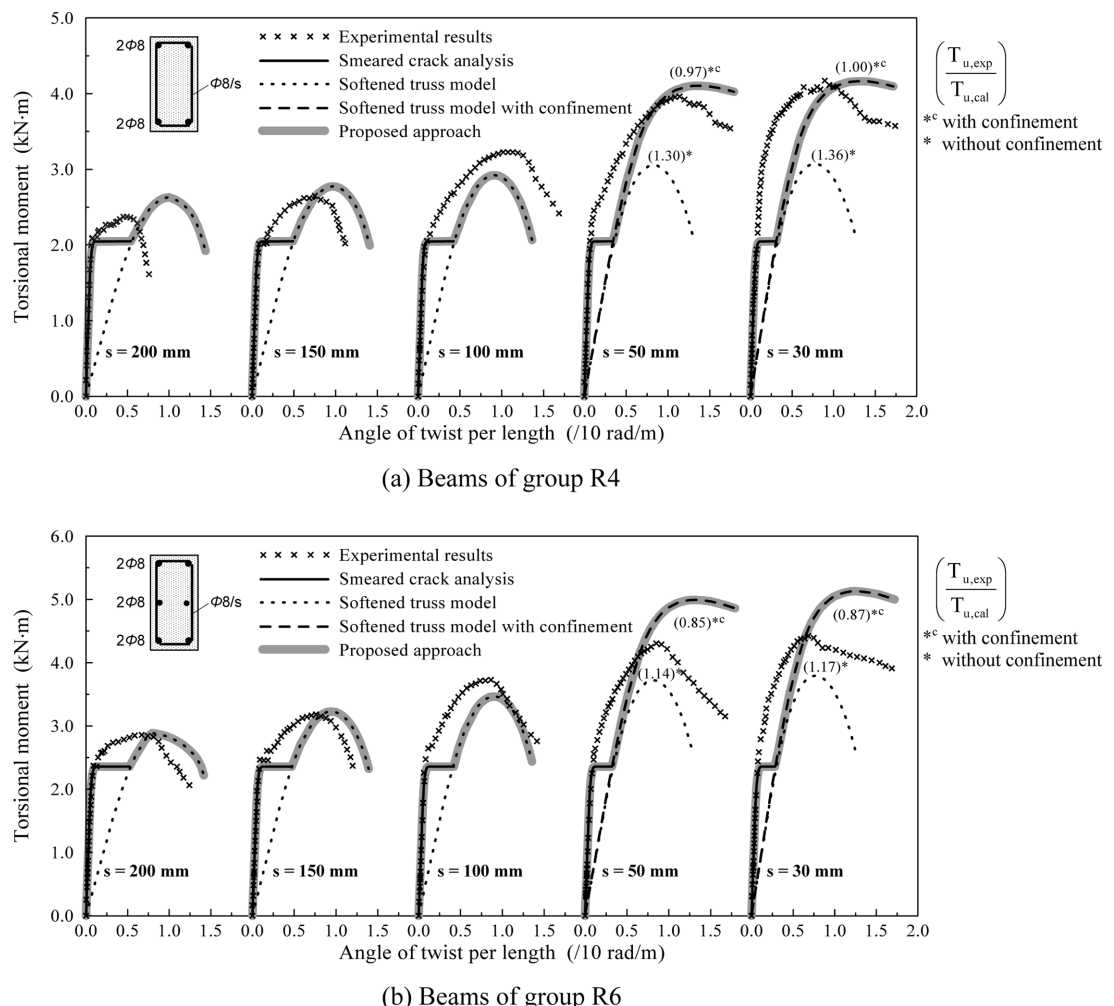


Fig. 10 Experimental and calculated T - θ curves for beams of series I

The calculated values of the torsional moment at cracking ($T_{cr,cal}$), the initial torsional stiffness (K_{cal}), the ultimate torsional moment ($T_{u,cal}$) and the corresponding angle of twist ($\vartheta_{Tu,cal}$) were calculated. These values are presented and compared with the measured ones in Table 5. From this

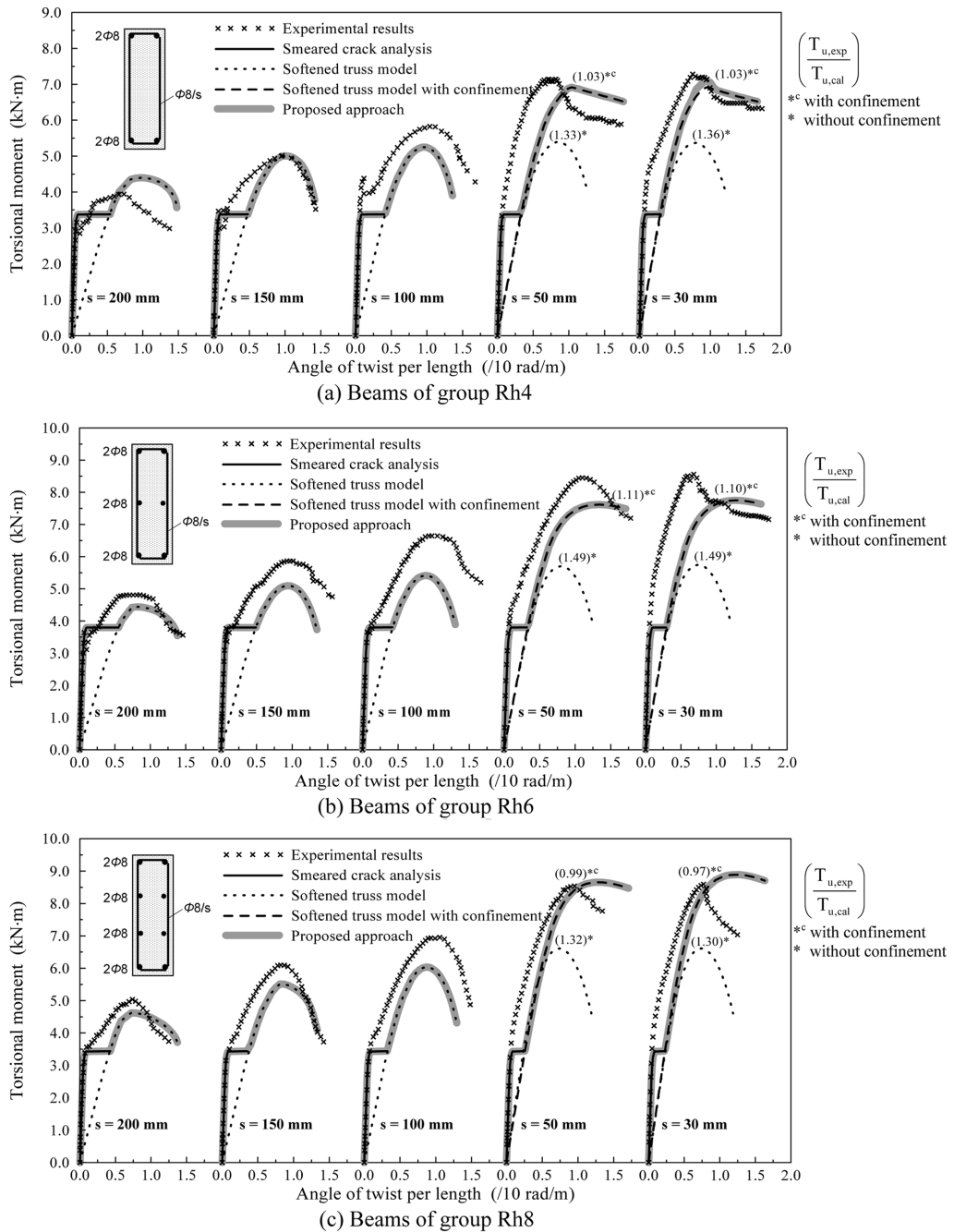


Fig. 11 Experimental and calculated T - ϑ curves for beams of series II

Table 6 Effect of the confinement in the softened truss model on the ultimate torsional strength of beams with high volume of transverse reinforcement ($\rho_t > 1.4\%$)

Beams code name	Calculated results using the softened truss model									
	Test results (post-cracking)				without confinement (Hsu and Mo 1985)			with confinement (proposed modification)		
	ρ_t (%)	f'_c (MPa)	$T_{u,exp}$ (kN·m)	$\vartheta_{Tu,exp}$ (rad/m)	$T_{u,cal}$ (kN·m)	$\frac{T_{u,exp}}{T_{u,cal}}$	$\vartheta_{Tu,cal}$ (rad/m)	$T_{u,cal}$ (kN·m)	$\frac{T_{u,exp}}{T_{u,cal}}$	$\vartheta_{Tu,cal}$ (rad/m)
<i>Tests of the present experimental study</i>										
R-r4-5	2.5	20.96	3.974	0.115	3.053	1.30	0.083	4.103	0.97	0.135
R-r4-3	4.1	20.96	4.172	0.089	3.072	1.36	0.077	4.165	1.00	0.133
R-r6-5	2.5	24.59	4.251	0.079	3.721	1.14	0.083	4.995	0.85	0.131
R-r6-3	4.1	24.59	4.443	0.072	3.804	1.17	0.078	5.131	0.87	0.124
Rh-r4-5	2.3	26.56	7.144	0.072	5.371	1.33	0.087	6.916	1.03	0.104
Rh-r4-3	3.8	26.56	7.331	0.078	5.407	1.36	0.080	7.103	1.03	0.095
Rh-r6-5	2.3	24.90	8.474	0.108	5.704	1.49	0.080	7.618	1.11	0.135
Rh-r6-3	3.8	24.90	8.559	0.068	5.758	1.49	0.074	7.753	1.10	0.127
Rh-r8-5	2.3	27.39	8.553	0.093	6.493	1.32	0.080	8.657	0.99	0.125
Rh-r8-3	3.8	27.39	8.594	0.077	6.611	1.30	0.074	8.893	0.97	0.127
<i>Mean (10 beams):</i>					—	1.325	—	—	0.992	—
<i>Standard deviation:</i>					—	0.112	—	—	0.087	—
<i>PCA tests (Hsu 1968)</i>										
B4	1.6	30.5	47.33	0.057	48.69	0.97	0.048	52.36	0.90	0.060
B5	2.1	29.0	56.15	0.062	50.38	1.11	0.045	57.70	0.97	0.061
B6	2.6	28.8	61.68	0.065	52.64	1.17	0.043	62.00	0.99	0.062
B8	2.6	26.8	32.54	-	31.41	1.04	0.051	33.59	0.97	0.065
D4	1.6	30.6	47.90	0.056	48.80	0.98	0.048	52.52	0.91	0.060
M4	1.4	26.5	49.59	0.058	44.62	1.11	0.046	48.14	1.03	0.058
M5	1.8	28.0	55.69	0.063	49.48	1.13	0.044	54.85	1.02	0.060
M6	2.1	29.4	60.10	-	53.32	1.13	0.043	59.54	1.01	0.062
I4	1.6	45.0	58.07	-	59.31	0.98	0.048	62.30	0.93	0.060
I5	2.1	45.0	70.72	0.054	69.70	1.01	0.049	76.68	0.92	0.065
I6	2.6	45.8	76.71	0.055	74.79	1.03	0.047	83.80	0.92	0.066
J4	1.6	16.8	40.67	0.058	31.29	1.30	0.042	34.34	1.18	0.054
G5	1.6	26.9	71.96	0.054	64.96	1.11	0.048	71.33	1.01	0.060
N4	1.4	27.3	15.70	0.089	13.67	1.15	0.074	14.59	1.08	0.084
K3	1.6	29.0	28.47	0.076	26.89	1.06	0.066	28.42	1.00	0.078
K4	2.3	28.6	35.02	0.086	29.15	1.20	0.060	32.28	1.08	0.078
C4	1.8	27.2	25.31	0.078	25.64	0.99	0.054	26.70	0.95	0.068
C5	2.4	27.2	29.71	0.085	27.90	1.06	0.051	30.23	0.98	0.069
C6	3.2	27.6	34.23	0.091	29.71	1.15	0.048	34.18	1.00	0.072
<i>Mean (19 beams):</i>					—	1.088	—	—	0.993	—
<i>Standard deviation:</i>					—	0.087	—	—	0.069	—
<i>(Fang and Shiau 2004)</i>										
H-20-20	2.0	78.50	239.0	0.047	232.0	1.03	0.043	247.2	0.97	0.049
N-20-20	2.0	35.50	158.0	0.043	134.0	1.18	0.032	147.0	1.07	0.047
<i>Total: Mean (31 beams):</i>					—	1.166	—	—	0.995	—
<i>Standard deviation:</i>					—	0.145	—	—	0.073	—

table it can be observed that the ratio $T_{cr, exp}/T_{cr, cal}$ for the examined beams has mean value $(T_{cr, exp}/T_{cr, cal})_{mean} = 1.070$ with standard deviation 0.111 and the ratio K_{exp}/K_{cal} has mean value $(K_{exp}/K_{cal})_{mean} = 1.057$ with standard deviation 0.150. Also, the ratio $T_{u, exp}/T_{u, cal}$ for the examined cases has mean value $(T_{u, exp}/T_{u, cal})_{mean} = 1.031$ with standard deviation 0.096.

Further, analytical torque curves for the torsional behaviour of the beams with uniformly distributed longitudinal bars and stirrups of series I and II are presented and compared with the experimental ones in Figs. 10 and 11, respectively. The analytical T - ϑ curves plotted in these figures have been yielded from (i) the smeared analysis (continuous line), (ii) the softened truss model (dotted line), (iii) the softened truss model with confinement (dashed line) and (iv) the proposed combination of these methods (grey thick line).

Moreover, in order to estimate the effectiveness of the proposed modification on the softened truss model, analytical curves derived from the original softened truss model (without confinement) and the modified one (with confinement) are also compared in Figs. 10 and 11 for the beams with high volume of stirrups (10 beams wherein $s = 30$ and 50 mm). Comparisons between the calculated results derived from these two analytical models and the experimental data of the tested beams with short spacing of stirrups are also presented in Table 6. From these comparisons it is concluded that in most of the examined cases the predictions of the ultimate torsional strength using the modified softened truss model with the confinement effect are more close to the experimental results than the predictions of the original softened truss model.

In general, from the comparisons in Figs. 10 and 11, a good agreement between the calculated and the experimental T - ϑ curves is observed. It is emphasized that the proposed approach, that employs the combination of two different methods, yields realistic torsional curves for the entire response of the element and calculates with satisfactory accuracy the initial torsional stiffness, the torque moment at cracking and the ultimate torque capacity (see also comparisons in Table 5).

7. Relevant experimental studies from literature

In order to extensively investigate the effect of the confinement on the torsional behaviour of reinforced concrete beams with high volume of stirrups and to check the accuracy of the proposed modification to the softened truss model, Table 6 has been drawn. In this Table, the experimental values of the ultimate torsional moment of 31 beams with ratio of transverse reinforcement greater than 1.4% are compared with the calculated results yielded from (i) the original softened truss model and (ii) the modified softened truss model that considers the influence of confinement.

The database compiled for the validation study of the proposed approach contains 31 specimens; 10 beams from the present experimental study and 21 beams from the literature. The torsional tests of the literature came from the milestone study of Hsu in 1968 at PCA Laboratories (19 beams) and a recent research of Fang and Shiao in 2004 (2 beams). The examined beams of these two studies have high volume of transverse steel reinforcement ($\rho_t > 1.4\%$) (see also values of ρ_t in Table 6). The ratio of the longitudinal reinforcement of the beams varies from 0.5% to 3.1%, whereas the cross-sections are square with dimensions 254×254 mm and rectangular with dimensions that range from 152×305 mm to 350×500 mm.

Based on the comparisons of the ultimate torsional moments in Table 6, for the 10 tests of the present experimental study, the average of $(T_{u, exp}/T_{u, cal})$ is 1.325 with standard deviation 0.112 for the predictions of the softened truss model without confinement, whereas for the predictions of the

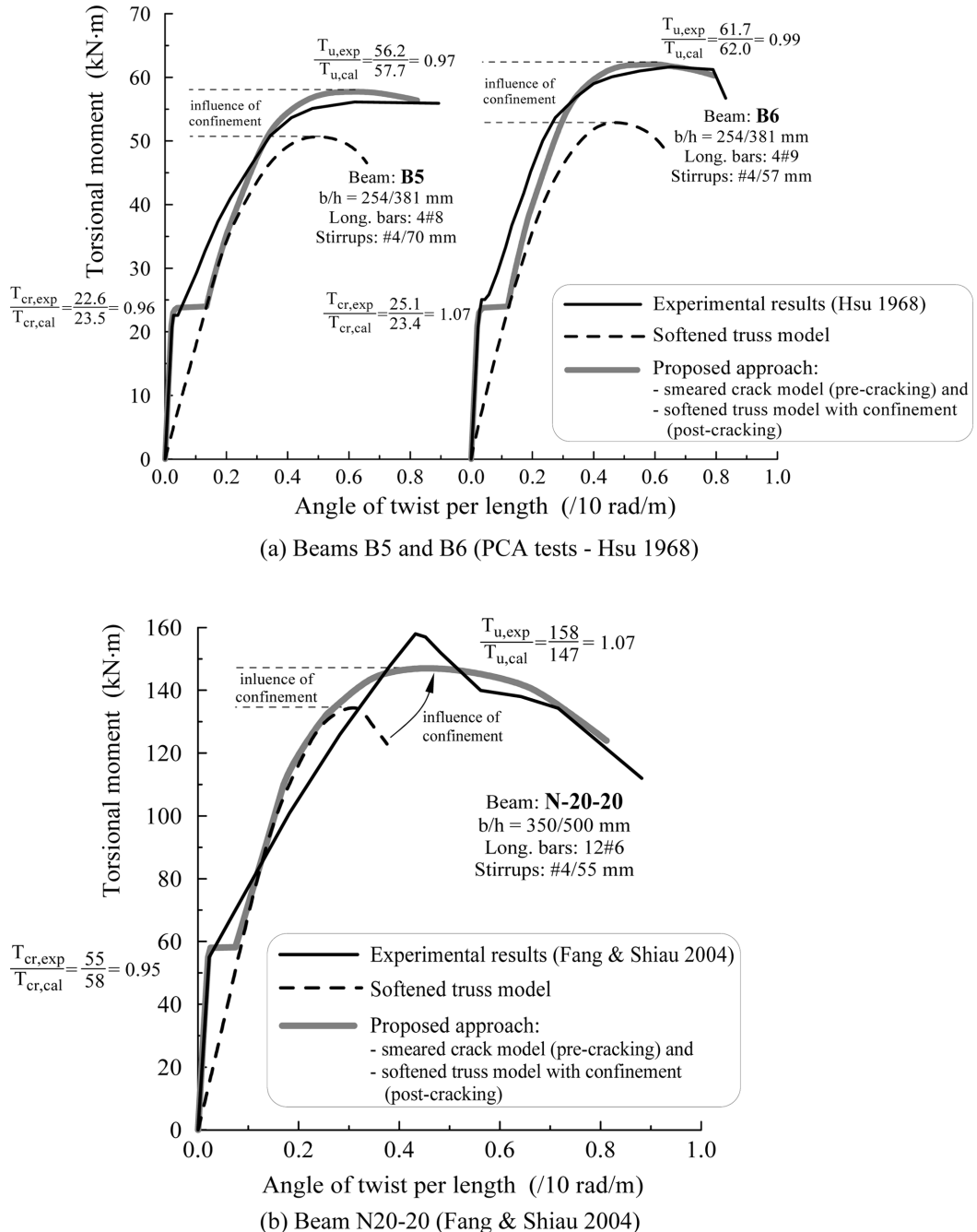


Fig. 12 Experimental and calculated T - ϑ curves using the proposed approach (with confinement) and the softened truss model for 3 beams of the literature

softened truss model with the proposed modification of the confinement effect the average of $(T_{u,\text{exp}}/T_{u,\text{cal}})$ is 0.992 with standard deviation 0.087. For the 19 PCA tests, these values are 1.088 and 0.087 for the predictions of the original softened truss model, whereas for the predictions of the

modified one they are equal to 0.993 and 0.069. Finally, for the total examined cases (31 beams) the average of $(T_{u,exp}/T_{u,cal})$ is 1.166 with standard deviation 0.145 for the predictions of the softened truss model without confinement, whereas for the predictions of the softened truss model with the proposed modification of the confinement effect these values are equal to 0.995 and 0.073. These results indicate that the proposed modification to the softened truss model in order to take into account the influence of the confinement significantly improves the accuracy of the model for the most of the beams with high volume of transverse steel reinforcement.

Further, Fig. 12 compares the entire experimental torsional behaviour and the calculated $T-\vartheta$ curves of the beams B5 and B6 of PCA tests (Hsu 1968) and the beam N-20-20 (Fang and Shiau 2004). The analytical $T-\vartheta$ curves have been calculated using (i) the softened truss model (dashed line) and (ii) the proposed combination of the smeared crack model for the pre-cracking and the modified softened truss model with confinement for the post-cracking (grey thick line). From these comparisons it is clear that the best fit throughout the pre-cracking and post-cracking response is achieved using the curve calculated by the proposed approach.

8. Conclusions

Experimental results of torsional tests on 56 reinforced concrete beams comprised various longitudinal and transverse reinforcement volumes and reinforcement arrangements have been reported. The following concluding remarks are drawn from the tests reported herein:

1. Volume of the transverse reinforcement significantly affects the torsional behaviour of the tested beams, as it was expected. Torque capacity increased with an increase in the value of volume of stirrups up to a value of 2.5%, however, the effect of transverse reinforcement decreases beyond this point.
2. Additional longitudinal steel bars increase the torsional strength of the tested beams. The influence of the longitudinal reinforcement decreases as more bars were added at the lower side of the stirrup (beams comprised unsymmetrical longitudinal reinforcement) and the volume of the transverse reinforcement is low.
3. Two distinct regions can be observed in a typical experimental torque – twist curve of the tested reinforced concrete beams. The different character of the response in these regions reveals the different nature of the load resisting mechanism in each case. In order to describe the entire torsional behaviour of the tested beams and based on the above observation, the combination of two different theories is adopted. For the estimation of the pre-cracking response a smeared crack analysis for plain concrete in torsion is used, whereas the prediction of the post-cracking behaviour is achieved using the softened truss model. Comparisons between the calculated torsional behaviour and the measured one show that the combined approach is capable to adequately describe the entire torsional response of reinforced concrete elements and to predict accurately the torsional moment at cracking and the ultimate torsional strength.
4. The influence of the confinement on the torsional behaviour of beams with high volume of transverse reinforcement is significant. Examination of existing experimental data indicated that the proposed modification to the well-known softened truss model in order to take into account the developed confinement of concrete due to the short spacing of stirrups yielded to accurate predictions of the ultimate torsional strength and post-cracking response.

References

- Ashour, S.A., Samman, T.A. and Radain, T.A. (1999), "Torsional behavior of reinforced high-strength concrete deep beams", *ACI Struct. J.*, **96**(6), 1049-1058.
- Belarbi, A. and Hsu, T.C. (1995), "Constitutive laws of softened concrete in biaxial tension-compression", *ACI Struct. J.*, **92**(5), 562-573.
- Chalioris, C.E. (1999), "Study of the behaviour and the failure mechanisms of plain and reinforced concrete elements in torsion", PhD dissertation, Department of Civil Engineering, Democritus University of Thrace, Xanthi, Greece.
- Chalioris, C.E. (2003), "Cracking and ultimate torque capacity of reinforced concrete beams", *Proc. of the Int. Symposia "Celebrating Concrete: People and Practice"*, University of Dundee, Scotland, UK, Vol. Role of Concrete Bridges in Sustainable Development, 109-118.
- Comité Euro-International du Béton – Fédération International de la Précontrainte (CEB-FIP) (1993), *Model Code 90 for Concrete Structures*, Thomas Telford, London.
- Fang, I.K. and Shiao, J.K. (2004), "Torsional behavior of normal- and high-strength concrete beams", *ACI Struct. J.*, **101**(3), 304-313.
- Hsu, T.C. (1968), "Torsion of structural concrete – Behavior of reinforced concrete rectangular members", *Torsion of Structural Concrete*, SP-18, American Concrete Institute, 261-306.
- Hsu, T.C. (1993), *Unified Theory of Reinforced Concrete*, CRC Press, Inc., Boca Raton, Fla.
- Hsu, T.C. (1996), "Toward a unified nomenclature for reinforced-concrete theory", *J. Struct. Eng.*, ASCE, **122**(3), 275-283.
- Hsu, T.C. and Mo, Y.L. (1985), "Softening of concrete in torsional members – Theory and tests", *ACI J., Proc.*, **82**(3), 290-303.
- Karayannidis, C.G. (2000a), "Smeared crack analysis for plain concrete in torsion", *J. Struct. Eng.*, ASCE, **126**(6), 638-645.
- Karayannidis, C.G. (2000b), "Nonlinear analysis and tests of steel-fiber concrete beams in torsion", *J. Struct. Eng. Mech.*, **9**(4), 323-338.
- Karayannidis, C.G. and Chalioris, C.E. (2000a), "Experimental validation of smeared analysis for plain concrete in torsion", *J. Struct. Eng.*, ASCE, **126**(6), 646-653.
- Karayannidis, C.G. and Chalioris, C.E. (2000b), "Strength of prestressed concrete beams in torsion", *Struct. Eng. Mech.*, **10**(2), 165-180.
- Mansur, M.A., Nagataki, S., Lee, S.H. and Oosumimoto, Y. (1989), "Torsional response of reinforced fibrous concrete beams", *ACI Struct. J.*, **86**(1), 36-44.
- Mitchell, D. and Collins, M.P. (1974), "Diagonal compression field theory – A rational model for structural concrete in pure torsion", *ACI J., Proc.*, **71**(8), 396-408.
- Rahal, K.N. and Collins, M.P. (1995), "Analysis of sections subjected to combined shear and torsion – A theoretical model", *ACI Struct. J.*, **92**(4), 459-469.
- Rahal, K.N. and Collins, M.P. (1996), "Simple model for predicting torsional strength of reinforced and prestressed concrete sections", *ACI Struct. J.*, **93**(6), 658-666.
- Rahal, K.N. and Collins, M.P. (2003), "Combined torsion and bending in reinforced and prestressed concrete beams", *ACI Struct. J.*, **100**(2), 157-165.
- Vecchio, F.J. and Collins, M.P. (1986), "Modified compression field theory for concrete elements subjected to shear", *ACI Struct. J.*, **83**(2), 219-231.
- Victor, D.J. and Muthukrishnan, R. (1973), "Effect of stirrups on ultimate torque of reinforced concrete beams", *ACI J., Proc.*, **70**(4), 300-306.
- Wafa, F.F., Shihata, S.A., Ashour, S.A. and Akhtaruzzaman, A.A. (1995), "Prestressed high-strength concrete beams under torsion", *J. Struct. Eng.*, ASCE, **121**(9), 1280-1286.

Notation

f_c'	: compressive strength of concrete cylinder
f_{sp}	: split concrete cylinder tensile strength
f_{ct}	: tensile strength of concrete
$f_{y\ell}$: yield strength of longitudinal steel bars
f_{yt}	: yield strength of transverse steel stirrups
ρ_ℓ	: steel ratio of longitudinal steel bars
ρ_t	: steel ratio of transverse steel stirrups
s	: spacing of steel stirrups
$T_{cr, exp}$: experimental torsional moment at cracking
$\vartheta_{cr, exp}$: experimental angle of twist per unit length at cracking
$T_{u, exp}$: ultimate experimental torsional moment
$\vartheta_{Tu, exp}$: experimental angle of twist per unit length at the ultimate torsional moment
K_{exp}	: experimental initial torsional stiffness
$T_{cr, cal}$: calculated torsional moment at cracking
$\vartheta_{cr, cal}$: calculated angle of twist per unit length at cracking
$T_{u, cal}$: ultimate calculated torsional moment
$\vartheta_{Tu, cal}$: calculated angle of twist per unit length at the ultimate torsional moment
K_{cal}	: calculated initial torsional stiffness
σ_{ct}	: tensile concrete stress
ε_{ct}	: total tensile concrete strain
ε^e	: elastic strain component for concrete in tension
ε^{fr}	: fracture strain component for concrete in tension
w	: crack width for concrete in tension
w_o	: crack width for a fully opened crack
E_{ct}	: modulus of elasticity of concrete in tension
G_f	: fracture energy in $\sigma_{ct} - w$ relationship
ℓ_w	: width of the fracture process zone for concrete in tension
α_f	: coefficient of the tensile concrete response in $\sigma_{ct} - w$ relationship
σ_d	: average compressive stress of the diagonal concrete struts
ε_d	: concrete compressive strain of the diagonal concrete struts
ε_o	: concrete compressive strain at ultimate stress of non-softened concrete (= 0.002)
ζ	: softening coefficient for concrete in compression
k	: confinement index
α	: confinement coefficient
ω_w	: mechanical ratio of the transverse reinforcement to the confined concrete core
$\varepsilon_{\zeta85}$: softened concrete strain at compressive stress equal to $0.85 \zeta f_c'$
$\varepsilon_{c\zeta85}$: maximum strain of softened and confined concrete